Chemical etching of a GaSb crystal incorporated with Mn grown by the Bridgman method under microgravity conditions*

Chen Xiaofeng(陈晓锋)[1,†], Chen Nuofu(陈诺夫)[1,2,†], Wu Jinliang(吴金良)[1,2], Zhang Xiulan(张秀兰)[1], Chai Chunlin(柴春林)[1], and Yu Yude(俞育德)[1]

(1 Key Laboratory of Semiconductor Materials and Devices, Institute of Semiconductors, Chinese Academy of Sciences, Beijing 100083, China)

(2 National Laboratory of Microgravity, Institute of Mechanics, Chinese Academy of Sciences, Beijing 100080, China)

Abstract: A GaSb crystal incorporated with Mn has been grown by the Bridgman method on the Polizon facility onboard the FOTON-M3 spacecraft. Structural defects and growth striations have been successfully revealed by the chemical etching method. By calculating various parameters of the convection, the striation patterns can be explained, and the critical value of the Taylor number, which characterizes the convective condition of the rotating magnetic field induced azimuthal flow, was shown. The stresses generated during crystal growth can be reflected by the observations of etch pit distribution and other structural defects. Suggestions for improving the space experiment to improve the quality of the crystal are given.

Key words: chemical etching; etch pit; defect; growth striations; convection

DOI: 10.1088/1674-4926/30/8/083006 **EEACC:** 2520

1. Introduction

Research on the incorporation of transition metals or rare earths into lattices of semiconductors to form diluted magnetic semiconductors (DMS) has gained a lot of interest in recent years with the development of spintronics. The discovery of carrier-induced ferromagnetism[1] in Mn-based DMSs has received much attention because of the potential device applications in which both information processing and data storage can be utilized within one material system.

Because of the nature of the low equilibrium solubility of magnetic irons in III–V semiconductors, non-equilibrium growth methods, such as molecular beam epitaxy (MBE), magnetic sputtering (MS), and chemical vapor deposition (CVD) are often adopted in order to incorporate magnetic irons into III–V materials beyond thermodynamic solubility limits. (Ga, Mn)Sb DMS grown by LTMBE was first reported in 2000[2]. Though experiments on the bulk growth of DMS materials under near equilibrium mode are relatively rare compared with non-equilibrium methods, Bridgman and Czochralski growth of GaSb doped with Mn have also been reported[3,4].

Many techniques have been used in the detection of defects, such as chemical etching, thermal etching, decoration technique and topographic techniques. Among the methods involving the examination of defects in crystals, the chemical etching technique is the method most widely used because of its reliability, speed and simplicity. Besides the detection of defects in the crystal, chemical etching can also detect growth striations from which the convection conditions during the crystal growth process can be reflected.

In this paper, we use the chemical etching technique to show the defects, etch pits, and growth striations of a GaSb crystal incorporated with Mn which was grown by the Bridgman method in space. A lot of information about the structure of the crystal is shown and the convective flow condition of the melt during growth can be known. The critical value of the Taylor number, which characterizes the rotating magnetic field (RMF) induced flow, can be obtained by a combination of the calculation of the flow parameters and observation of the striation patterns.

2. Experiment

2.1. Crystal growth

High purity gallium (99.9999%), antimonide (99.9999%), and manganese (99.99%) are used in our experiment. Prior to the space experiment, the materials were first mixed and melted on earth in a crucible by the vertical gradient freezing (VGF) method. A single crystal GaSb grown by the liquid encapsulated Czochralski (LEC) method was used as a seed and the (100) face of the seed for contacting with the feed crystal was chemically polished previously. Before filling it with the materials, the silica crucible was carefully cleaned and finally the material-filled crucible and shockproof graphite blocks were filled in a bigger ampoule and sealed to get a near-vacuum inner ambient.

The space experiment was carried out in the multi-zone

* Project supported by the Space Agency of China and the Chinese Academy of Sciences.

† Corresponding author. Email: xfchen@semi.ac.cn, nfchen@semi.ac.cn

Received 2 March 2009

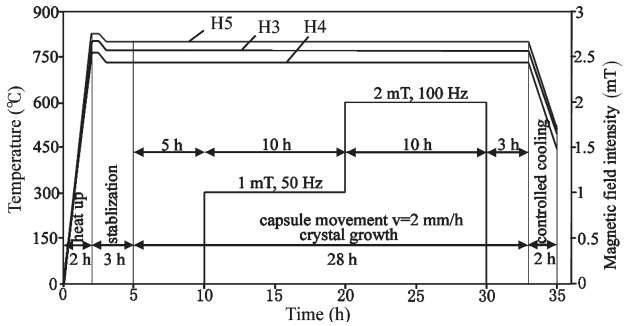

Fig. 1. Cyclogram of the GaMnSb crystal growth experiment.

Polizon furnace located in the Russian Foton-M3 spacecraft in September 2007. A detailed scheme of the furnace can be found in Ref. [5]. In our experiment, only the heaters H3, H4, H5 are active and by modulating the temperatures of these heaters the temperature gradient of the solid-melt boundary in the furnace was controlled to be 10 ± 2 °C/cm in our experiment.

Figure 1 shows a cyclogram of the space experiment, from which the experiment can be described by the following steps. Firstly the furnace was heated up by these heaters for 2 h, and then a 3-hour stabilization period followed to achieve the designed temperature distribution along the furnace. Next, a 28-hour growth step which can be divided into four distinct stages under a constant pulling rate of 2 mm/h followed. At first, the growth process took place under microgravity conditions without any external magnetic field for 5 h. After that, a rotating magnetic field (RMF) with an intensity of 1 mT and a frequency of 50 Hz was introduced and this stage lasted for 10 h. Thirdly, the parameters of the RMF were changed to an intensity of 2 mT and a frequency of 100 Hz, and this stage also lasted for 10 h. The last growth stage took place without any RMF and lasted for 3 h. At the end of the growth process a step of 2-hour controlled cooling took place.

After growth, the crystal ingot was taken out of the ampoule and mechanically cut parallel to the central axis along the (100) growth direction to get a 0.5 mm thick (110)-oriented slice and mechanically polished to remove the cutting scratches in order to perform the chemical etching experiment.

2.2. Chemical etching

From the chemical point of view, the etchant for the etching of semiconductor materials involves the following ingredients: oxidants (like $KMnO_4$, H_2O_2, HNO_3, and Br_2) which react with the material in the surface to form the oxide, solvents (like HF, HCl, HBr, and H_3PO_4) which dissolve the oxide, and medium reagents (like H_2O, CH_3COOH, and CH_3OH) which provide the medium for the reaction. Common etchants used for the detection of etch pits and growth striations are listed in Ref. [6, 7].

To display the growth striations in our material, etching with $KMnO_4$ (saturated): HF: CH_3COOH at room temperature for about 20 min was applied. Prior to this process chemical polishing with HF: $9HNO_3$: $20CH_3COOH$ for about 1 min was needed. It should be noted that after the chemical polishing the slice should be immediately taken into the striation revealing etchant to avoid contact with the air. Otherwise, a gray oxide film can be formed and further influence the effect of the striation etching. Besides, the etching of striations should be in a stationary environment, not stirring and shaking, in order to decrease the surface undulation.

For the detection of the etch pits, etching with $2HNO_3$: HF: $2CH_3COOH$ at room temperature for 10 s was applied. Chemical polishing with HF: $9HNO_3$: $20CH_3COOH$ for about 45 s was also needed prior to the etch pit displaying process.

3. Results and discussion

3.1. Striations

Figure 2(a) gives an image of the slice after rubbing away the cutting scratches and Figure 2(b) shows a schematic diagram of the striations revealed in the slice. The regions marked as numbers in Fig. 2(b) correspond to the different growth stages, which are shown in Fig. 1. It can be seen in Fig. 2(a) that the 0–30 mm part is single crystal, and the grain boundary was introduced at 30 mm from the upper side of the slice and extends toward the tail. The striation distribution is inhomogeneous, as shown in Fig. 2(b). Figure 3 represents two differential interface contrast microscopy images of the growth striations. Figure 3(a) is taken from the border between regions 1 and 2 as marked in Figs. 2(b) and 3(b) is taken from the border between regions 2 and 3.

To explain the observed striation patterns, it is necessary to analyze the convection of our system. Three kinds of convection dominate in our system: buoyancy-driven convection, surface tension driven convection and RMF induced forced azimuthal swirling flow. To describe these convections, we have to calculate the Rayleigh number, the Marangoni number and the Taylor number of our system, where the Rayleigh number, Ra, describes the buoyancy-driven convection, the Marangoni number, Ma, describes the surface tension driven convection, and the Taylor number, Ta, describes the RMF driven convection. It is believed that when the parameter of one kind of convection is small this convection is time-independent, or steady; and when this parameter exceeds the critical value the convection becomes time-dependent, or turbulent. When the convection is time-dependent, the temperature at the solid-melt boundary fluctuates and hence striations appear. The parameters used in our calculation are listed in Table 1[8].

The Rayleigh number

$$\mathrm{Ra} = g\beta\Delta T H^3/\nu\kappa \tag{1}$$

describes buoyancy-driven convection. In microgravity conditions where the gravitational acceleration is 6 magnitudes lower than the terrestrial value, Ra is extremely small (Ra = 2.3) that buoyancy-driven convection cannot occur because the critical Rayleigh number in such an aspect ratio is about

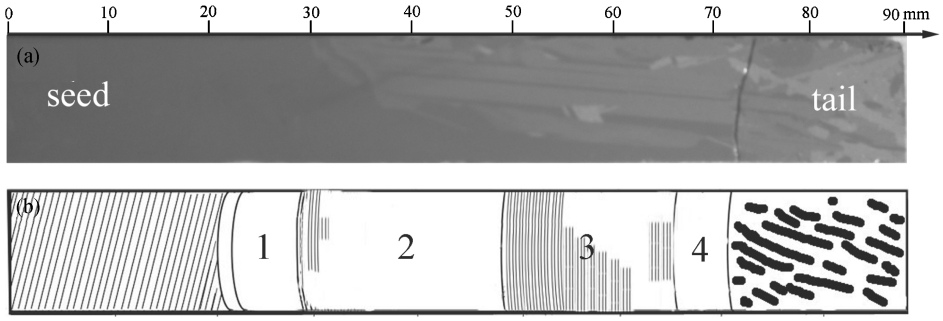

Fig. 2. (a) Image of the slice taken from the crystal; (b) Schematic diagram of the striations revealed in the slice.

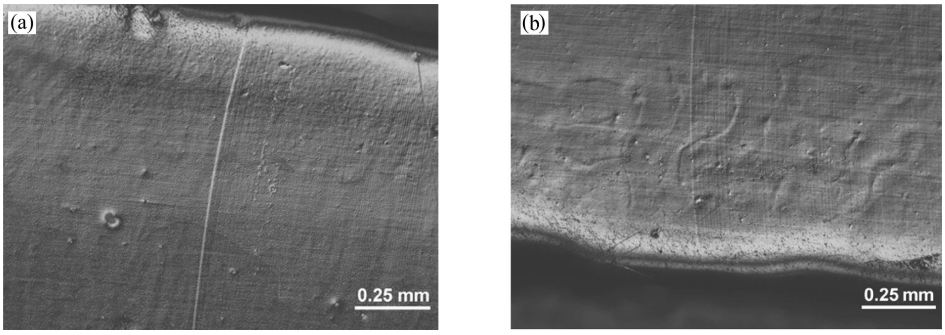

Fig. 3. Microscopic images of the striations revealed in the crystal.

Table 1. Parameters used in the calculation of convections.

Parameter	Value
Melt density ρ (g/cm^3)	6.03
Kinematic viscosity ν (cm^2/s)	0.00383
Dynamic viscosity $\eta = \rho\nu$ (g/(cm·s))	0.0231
Thermal diffusivity κ (cm^2/s)	0.087
Heat conductivity k (W/(cm·K))	0.171 (melt), 0.0781 (solid)
Volume expansion coefficient β (K^{-1})	9.58×10^{-5}
Prandtl number Pr	0.044
Gravitational acceleration g (m/s^2)	$10^{-6} g_0$ (measured)
Electrical conductivity σ (Ω·m)$^{-1}$	1.0×10^6[9]
Melt height H (mm)	65 (first growth stage)
ΔT (K)	30 (for Ra), 10 (for Ma)
Radius R (mm)	6
Surface tension gradient $\partial\gamma/\partial T$ (N/mK)	-1×10^{-4}[10]
Free surface length l (mm)	10

10^5–10^6[11, 12]. With the growth of the crystal, the melt height becomes shorter, and hence a smaller value of Ra is obtained during the rest stages. Consequently, the formation of striations can not be attributed to buoyancy-driven convection and this is why in part 1 and part 4 no striations are observed.

Because of the microgravity, the free surface detached from the ampoule wall during crystal growth and hence surface tension driven flow, Marangoni flow, appears. There are two critical Marangoni numbers: Ma_{c1}—critical Marangoni number for the transition to a 3-D configuration, and Ma_{c2}—critical Marangoni number for the transition to time-dependent convection. The value of Ma_{c2} can be calculated by two different empirical formulas given in the following:

$$\begin{cases} \mathrm{Ma}_{c2} = 6.9 \times 10^4 \times \mathrm{Pr}^{1.36}, & \mathrm{Pr} \ll 1, \\ \mathrm{Ma}_{c2} = 2.6 \times 10^3 \times \mathrm{Pr}^{0.69}, & \mathrm{Pr} \gg 1 \text{[8]}. \end{cases} \quad (2)$$

$$\mathrm{Ma}_{c2} = 2.2 \times 10^4 \times \mathrm{Pr}^{1.32}\text{[10]}. \quad (3)$$

For GaSb, the values of the calculated Ma_{c2} are 986.2 and 356.3 respectively. In the present experiment, the free surface length is found to be about 10 mm, and the Marangoni number

$$\mathrm{Ma} = -(\partial\gamma/\partial T)(\Delta T l)/\eta\kappa \quad (4)$$

is calculated to be 500. Actually, no any striations can be observed in the regions with free surface (from about 33 to 45 mm), indicating that Eq. (1) is more suitable. Thus, surface tension driven flow is not the cause of the striations.

The introduction of RMF leads to a Lorentz force and hence a forced azimuthal swirling flow occurs. This forced convection is characterized by the Taylor number

$$\mathrm{Ta} = B^2 R^4 \omega\sigma\rho/2\eta^2. \quad (5)$$

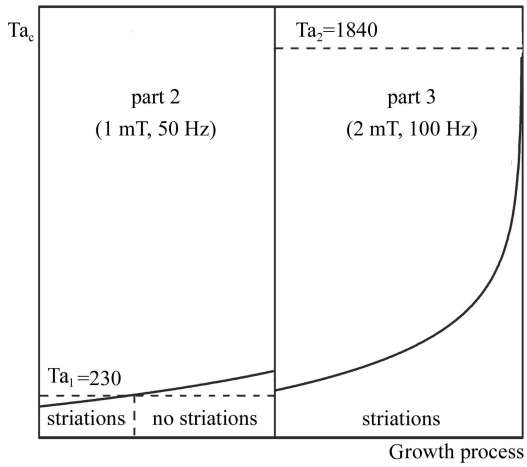

Fig. 4. Relationship between Ta_c and growth process.

According to this expression, Ta is independent of melt height and gravitation, so Ta is constant for a fixed magnetic field. In the present experiment, the values of Ta are calculated to be 230 and 1840 for the second (with RMF of 1 mT, 50 Hz) and the third stages (with RMF of 2 mT, 100 Hz) of growth, respectively. The previous results demonstrated that Ta_c decreases with increasing aspect ratio[13, 14] or magnetic field frequency (Reynold number)[13]. In this experiment, on the one hand, the aspect ratio continually decreases as crystal growth progresses. On the other hand, the magnetic field frequency increases from 50 Hz in the second stage to 100 Hz in the third stage. Therefore, two opposite effects on Ta_c have to be considered to understand the striation patterns.

From Fig. 2(b) it can be seen that the striations in part 2 last for a short length and after 30 mm the striations gradually become weak and disappear. As mentioned before, Ta is constant (Ta_1 = 230) in this stage, but the critical Taylor number increases since the aspect ratio (melt height compared with melt radius) became smaller. So the disappearance of the striations at about 30 mm indicates that Ta_c is below Ta before 30 mm and Ta_c becomes higher than Ta after 30 mm. In part 3, with a RMF of 2 mT and 100 Hz, striations can be seen all along this part, implying that Ta_c is kept below Ta throughout this part. On the one hand, during the transition from stage 2 to stage 3, the frequency of RMF increases, so Ta_c abruptly decreases at the boundary since the frequency has an influence on Ta_c. On the other hand, during stage 3 Ta_c is also increasing as the aspect ratio decreases, but the value of Ta_c never exceeds Ta (Ta_2 = 1840).The above relations of Ta_c relative to the growth process in stages 2 and 3 are illustrated in Fig. 4.

3.2. Etch pits and other defects

The etch pits in the crystal were detected by our etching process. Figure 5 represents images of two typical etch pits, from which we can see that the etch pit in Fig. 5(a) is symmetrical and the one in Fig. 5(b) is asymmetrical.

The etch pit distribution in the slice is inhomogeneous since the periphery of the slice has a higher etch pit density (as much as 1000 cm^{-2}) compared with the central part (about 40 cm^{-2}).

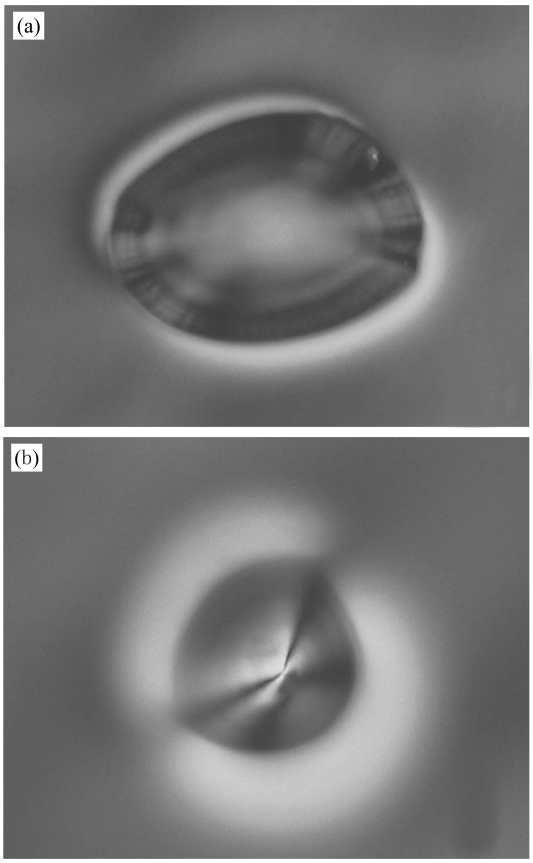

Fig. 5. Images of two typical etch pits.

During the etching of the growth striations, other defects, such as grain boundaries and facets, were also presented. Figure 6 shows two defects in our crystal. In Fig. 6(a), the grain boundaries originated from the upper side of the slice and extended toward the inside of the crystal. In Fig. 6(b), this structure also formed in the periphery of the crystal and developed into the inside of the crystal.

The defects and the inhomogeneous distribution of the etch pits indicate that during the crystal growth process, strong stresses are introduced and this is one of the causes of the formation of dislocations and other defects. The density of melt GaSb is 6.03 g/cm^3, larger than the density of solid GaSb (5.61 g/cm^3), and when transformed from melt to solid the volume expanded toward the crucible inner wall and high stress was generated.

4. Conclusion

A GaSb crystal incorporated with Mn was grown by the Bridgman method in space. Growth striations, etch pits, and other defects of the crystal were successfully revealed by chemical etching. The convections in the melt were analyzed and the inhomogeneous distribution of the striations was explained. The etch pit distribution and other defects reflect the stress conditions of the growth experiment.

To eliminate the striations the parameters of the RMF should be carefully chosen and to reduce the stresses during

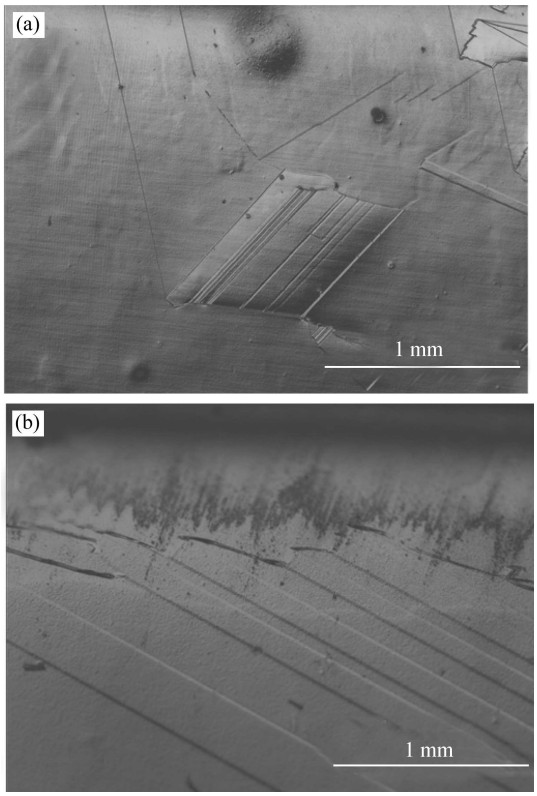

Fig. 6. Two defect structures in the crystal.

crystal growth some kind of detached growth methods (like the floating zone technique) should be utilized, especially in the growth of crystals with high expansion ratios.

Acknowledgement

The authors would like to give many thanks to the colleagues at the Design Bureau of General Machine-Building, Russian Aviation and Space Agency.

References

[1] Ohno H. Properties of ferromagnetic III–V semiconductors. J Magn Mater, 1999, 200: 110

[2] Matsukura F, Abe E, Ohno H. Magnetotransport properties of (Ga, Mn)Sb. J Appl Phys, 2000, 87: 6442

[3] Sestakova V, Hubik P, Stepanek B, et al. GaSb single crystals doped with manganese. J Cryst Growth, 1993, 132: 345

[4] Adhikari T, Basu S. Electrical properties of gallium manganese antimonide: a new diluted magnetic semiconductor. Jpn J Appl Phys, 1994, 33: 4581

[5] Serebryakov Y A, Prokhorov I A, Vlasov V N, et al. Concentration and structure inhomogeneities in GaSb(Si) single crystals grown at different heat and mass transfer conditions. J Cryst Growth, 2007, 304: 11

[6] Dutta P S, Bhat H L, Kumar V. The physics and technology of gallium antimonide: an emerging optoelectronic material. J Appl Phys, 1997, 81: 5821

[7] Clawson A R. Guide to references on III–V semiconductor chemical etching. Mater Sci Eng R, 2005, 31: 1

[8] Müller G, Ostrogorsky A. Convection in melt growth. In: Hurle D T J. Handbook of crystal growth. Chap 13. Amsterdam: Elsevier, 1993

[9] Glazov V M, Chizhevskaya S N, Glagoleva N N. Liquid semiconductors. New York: Plenum Press, 1969

[10] Cröll A, Kaiser T, Schweizer M, et al. Floating-zone and floating-solution-zone growth of GaSb under microgravity. J Cryst Growth, 1998, 191: 365

[11] Müller G, Neumann G, Weber W. Natural convection in vertical Bridgman configurations. J Cryst Growth, 1984, 70: 78

[12] Müller G, Neumann G, Matz H. A two-Rayleigh-number model of buoyancy-driven convection in vertical melt growth configurations. J Cryst Growth, 1987, 84: 36

[13] Mößner R, Gerbeth G. Buoyant melt flows under the influence of steady and rotating magnetic fields. J Cryst Growth, 1999, 197: 341

[14] Volz M P, Walker J S, Schweizer M, et al. Bridgman growth of germanium crystals in a rotating magnetic field. J Cryst Growth, 2005, 282: 305